

# Pinned Low Energy Electronic Excitation in Metal Exchanged Vanadium Oxide Nanoscrolls

J. Cao,<sup>1</sup> J. L. Musfeldt,<sup>1,\*</sup> S. Mazumdar,<sup>2</sup> N. Chernova,<sup>3</sup> and M. S. Whittingham<sup>3</sup>

<sup>1</sup>*Department of Chemistry, University of Tennessee, Knoxville, Tennessee 37996-1600*

<sup>2</sup>*Department of Physics, University of Arizona, Tucson, Arizona 85721*

<sup>3</sup>*Department of Chemistry and Institute for Materials Research, State University of New York, Binghamton, New York 13902-6000*

(Dated: November 17, 2018)

We measured the optical properties of mixed valent vanadium oxide nanoscrolls and their metal exchanged derivatives in order to investigate the charge dynamics in these compounds. In contrast to the prediction of a metallic state for the metal exchanged derivatives within a rigid band model, we find that the injected charges in  $\text{Mn}^{2+}$  exchanged vanadium oxide nanoscrolls are pinned. A low-energy electronic excitation associated with the pinned carriers appears in the far infrared and persists at low temperature, suggesting that the nanoscrolls are weak metals in their bulk form, dominated by inhomogeneous charge disproportionation and Madelung energy effects.

The discovery that low-dimensional inorganic solids can curve or fold into nanoscale objects provides an exciting opportunity to investigate bulk versus nanoscale chemistry using molecular-level strain as the tuning parameter.<sup>1,2,3</sup> These materials are targets of intensive research efforts, driven by the need to further miniaturize electronic devices and the potential to exploit unusual mechanical and optical properties. Some of the beautiful, flexible, and functional nanomorphologies include tubes, wires, octahedra, particles, urchins, and spheres.<sup>1,2,3,4,5,6,7,8,9</sup> They offer molecular-level control of size, shape, mechanical response, and chemical composition as well as unusual confinement effects due to finite length scales.

Among the transition metal oxides, vanadates show particularly rich chemistry due to the tunable vanadium oxidation state and flexible coordination environment, which ranges from octahedral to square pyramidal to tetrahedral with increasing vanadium oxidation state.<sup>10</sup> Vanadium oxides form many layered and nanoscale compounds with open structural frameworks, making them prospective materials for ion intercalation, exchange and storage.<sup>7,8,9,11</sup> The nanoscale vanadates of interest here,  $(\text{amine})_y\text{VO}_x$ , are formally mixed-valent<sup>6</sup> with  $x \sim 2.4$  and  $y \sim 0.28$ . Stoichiometric considerations do not, of course, distinguish between a true mixed-valent  $\text{V}^{4.5+}$  state that may be metallic and a state with an inhomogeneous charge distribution, consisting of V-ions with distinct small and large charges. Such charge disproportionation is common in oxides of Ti and V with formal oxidation states of  $\text{Ti}^{3.5+}$  and  $\text{V}^{4.5+}$ , respectively, and the convention is to assign integer charges ( $\text{Ti}^{3+}$  and  $\text{Ti}^{4+}$ ;  $\text{V}^{4+}$  and  $\text{V}^{5+}$ ) to the ions with different oxidation states.<sup>12,13,14</sup> We adopt the same convention here, and consider the possibility of charge disproportionation in the nanoscale vanadates.

The compounds we consider are actually scrolls, consisting of vanadate layers between which organic molecules are intercalated.<sup>6,7,8,15,16</sup> The size of the amine or diamine template determines scroll winding, providing

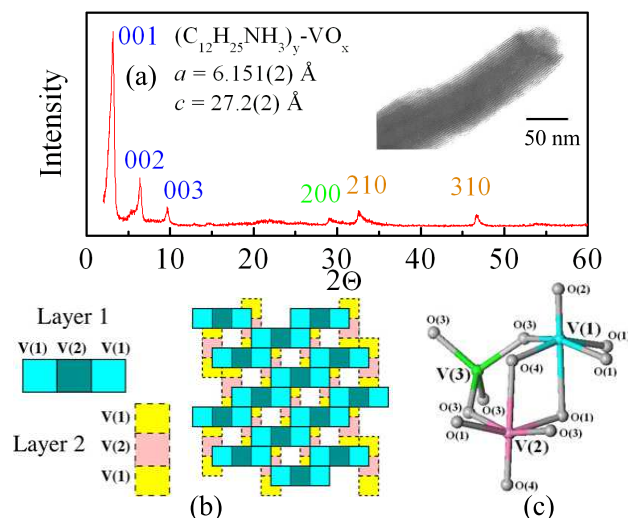


FIG. 1: (color online) (a) Representative x-ray powder diffraction scan of  $(\text{C}_{12}\text{H}_{25}\text{NH}_3)_y\text{-VO}_x$  scrolls showing only 00l and weak hk0 reflections. The inset displays a representative TEM image with lattice fringing and a center cavity. (b) Probable double-layer structure of the  $\text{VO}_x$  scrolls, analogous to the  $\text{BaV}_7\text{O}_{16}$  model compound.<sup>17</sup> (c) Close-up view of the local structure around the V centers, showing the arrangement of octahedra and tetrahedra in the  $\text{BaV}_7\text{O}_{16}$  model compound.<sup>17</sup>

an opportunity to tune the size of these materials. The typical scrolls are  $\sim 15\text{-}100$  nm in diameter, containing up to 30 vanadium oxide layers (inset of Fig. 1(a)). The exact crystal structure is complicated and is not completely understood. Figure 1(a) shows a representative x-ray powder diffraction pattern for the  $(\text{C}_{12}\text{H}_{25}\text{NH}_3)_y\text{-VO}_x$  scrolls. The (00l) reflections from the vanadium oxide layers are clear, but the (hk0) reflections from the atomic structure within each layer are weak. The data suggest a tetragonal lattice of basal repeat size  $6.144 \text{ \AA}$ , closely related to that of  $\text{BaV}_7\text{O}_{16}$ , which has a planar structure

of basal size 6.160 Å.<sup>17</sup> The arrangement in BaV<sub>7</sub>O<sub>16</sub> is shown in Fig. 1(b).<sup>17</sup> It contains zig-zag chains of edge-sharing VO<sub>5</sub> square pyramids. These chains share some corners with each other to form a two dimensional sheet. The sheets also share corners with VO<sub>4</sub> tetrahedra, bringing the two VO<sub>x</sub> layers together to form a characteristic double sheet. Figure 1(c) displays the local structure around the V centers in the BaV<sub>7</sub>O<sub>16</sub> model compound. Each two-dimensional layer contains two octahedrally coordinated vanadium atoms, V(1) and V(2), with one tetrahedrally coordinated V(3) occurs in between the layers.

Scrolled vanadates exhibit very interesting physical properties including a large spin gap, diameter-dependent optical features, and potential battery and optical limiting applications.<sup>18,19,20,21,22</sup> Recently, electron- and hole-doped vanadium oxide nanoscrolls were reported to be 300 K ferromagnets, raising fundamental questions about the underlying magnetic exchange mechanism.<sup>19</sup> It was further suggested that charge-injection via “doping” introduces free carriers into the pristine Mott insulating scrolls, resulting in partially filled bands. The “doped” nanoscrolls are predicted to exhibit Drude-type metallic behavior within this picture.<sup>19</sup> Direct measurement of the low-energy electronic structure is clearly important to test this prediction. Further, the rigid band model raises fundamental questions about the chemical nature of the “doping” or ion exchange process in the scrolled vanadates.<sup>16,19,23,24</sup> From the chemical perspective, metal intercalation does not appear as simple as “putting in electrons”; both reduction of vanadium as well as ion exchange with the proton on the amine are possible consequences of the exchange process. To date, only Mn<sup>2+</sup> has been shown to completely replace the organic template, even though some other ions such as Na<sup>+</sup>, Li<sup>+</sup>, Zn<sup>2+</sup>, Cu<sup>2+</sup>, and Ca<sup>2+</sup> can partially replace the amine template.<sup>16,23,24</sup>

In order to understand the fundamental charge dynamics and test the applicability of the rigid band model in vanadium oxide nanoscrolls, we investigated the variable temperature optical spectra of the pristine and Mn<sup>2+</sup> exchanged materials. In contrast to the rigid band model expectation for a metallic state, we find that charge is pinned in the metal substituted scrolls. The low-energy electronic excitation associated with the pinned carriers appears in the far infrared and persists at low temperature, suggesting that the nanoscrolls are weak metals in their bulk form, dominated by inhomogeneous charge disproportionation and Madelung energy effects. We propose an alternate model for charge injection to account for our observations. Analysis of the vibrational properties shows that the 575 cm<sup>-1</sup> V-O-V equatorial stretching mode is very sensitive to metal substitution, indicating that ion exchange modifies both the local curvature and charge environment. Charge effects also shift excitations in the higher energy optical conductivity.

Vanadate nanoscrolls were prepared by an initial sol-gel reaction followed by hydrothermal treat-

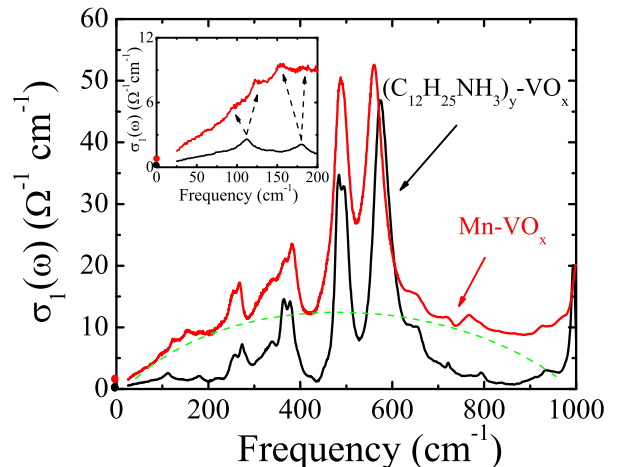


FIG. 2: (color online) 300 K optical conductivity of pristine VO<sub>x</sub> scrolls and the Mn<sup>2+</sup> exchanged compound in the far-infrared regime. Mode assignments include: V-O axial stretching at 945 and 995 cm<sup>-1</sup>, weak V-O-V equatorial stretching at 790 and 866 cm<sup>-1</sup>, V-O-V equatorial stretching at 585, 652, and 727 cm<sup>-1</sup>, V-O-V axial stretching at 486 and 498 cm<sup>-1</sup>, V-O bending at between 179 and 381 cm<sup>-1</sup>, and screw-like motion of the scroll at 113 cm<sup>-1</sup>.<sup>18</sup> The dashed green line guides the eye, highlighting the additional localized carrier contribution in the substituted scrolls. The inset shows a magnified view of the low-frequency response of pristine and Mn<sup>2+</sup> exchanged scrolls. The extrapolated dc conductivity is indicated by filled circles at  $\omega = 0$  in both panels.

ment, as described previously.<sup>18,23</sup> Appropriate amines (C<sub>n</sub>H<sub>2n+1</sub>NH<sub>2</sub> with  $n=4 - 18$ ) were employed as the structure-directing agent. Ion exchange was preformed by stirring a mixture of vanadate nanoscrolls and MCl<sub>2</sub> (M=Mn<sup>2+</sup>, Zn<sup>2+</sup>, and Na<sup>+</sup>) for 2 hours in ethanol/water mixture. The spectroscopic experiments were carried out over a wide energy range (4 meV - 6.2 eV; 30 - 50000 cm<sup>-1</sup>) using a series of spectrometers.<sup>18</sup> Variable temperature work was done between 4.2 and 300 K using an open-flow helium cryostat and temperature controller. The optical constants were calculated by a Kramers-Kronig analysis of the measured reflectance:  $\tilde{\epsilon}(\omega) = \epsilon_1(\omega) + i\epsilon_2(\omega) = \epsilon_1(\omega) + \frac{4\pi i}{\omega} \sigma_1(\omega)$ .<sup>25</sup>

Figure 2 shows the optical conductivity of the pristine VO<sub>x</sub> scrolls and the Mn<sup>2+</sup> substituted compounds at room temperature. The pristine scrolls display semi-conducting behavior, with clearly resolved vibrational modes below 1000 cm<sup>-1</sup> and a low background conductivity. These modes were previously assigned as V-O-V axial and equatorial stretching, V-O bending, and screw-like motion of the scrolls.<sup>18</sup> Subtle spectral changes occur when the amine template is exchanged for Mn<sup>2+</sup>, Zn<sup>2+</sup>, or Na<sup>+</sup>. In the Mn<sup>2+</sup> substituted compound (Fig. 2), the optical conductivity develops a broad electronic back-

ground in the far infrared region, with strong phonons riding top of this excitation. The Fano-like lineshapes of several phonons, especially those near  $250$  and  $380\text{ cm}^{-1}$ , indicate that the background is electronic in nature.<sup>26</sup> This localized electronic excitation has a width of  $\sim 400 - 500\text{ cm}^{-1}$ . Extrapolating  $\sigma_1(\omega)$  to zero frequency, we find  $\sigma_1(0) \sim 1\text{ }\Omega^{-1}\text{ cm}^{-1}$ . Such a pinned carrier response is characteristic of a weak or “bad” metal rather than a traditional Drude metal and has been observed in other complex oxides.<sup>27,28,29,30</sup> We obtain similar results at low temperature, suggesting that the vanadium centers in both pristine and ion-exchanged scrolls are charge disproportionated, with  $\text{V}^{4+}$  and  $\text{V}^{5+}$  centers rather than the mixed valent state ( $\text{V}^{4.5+}$ ) that might be anticipated for a highly conducting material.

Based on the observation of a pinned electronic excitation in the far infrared, the ion exchange processes does add carriers to the scrolled vanadates. The carriers are not, however, mobile in the ion substituted scrolls. Single scroll scanning tunneling microscope measurements are in progress to complement this spectroscopic work with local  $dI/dV$  measurements. Previous individual tube measurements of  $\text{Li}^+$  exchanged scrolls actually showed a decrease in conductivity with  $\text{Li}^+$  hole doping.<sup>19</sup>

We now discuss the evolution of the electronic structure of the nanoscrolls due to the metal exchange process within a heuristic correlated-electron model. We use an “effective” band picture, even though a localized description may be more suitable for charge-disproportionated V-oxides,<sup>31</sup> in order to maintain continuity with the existing literature.<sup>19</sup> The pristine scrolls, depicted in Fig. 3(a), are semiconductors with an optical gap of  $\sim 0.5\text{ eV}$ .<sup>18</sup> This gap derives from a superposition of both V on-site  $d$  to  $d$  excitations and  $\text{V}^{4+}$  to  $\text{V}^{5+}$  charge transfer excitations.<sup>18</sup> Thus charge disproportionation exists already in the pristine material. Optical gaps with similar magnitude are observed in bulk  $\text{VO}_2$ , ladder-like  $\alpha'\text{-NaV}_2\text{O}_5$ , tubular  $\text{Na}_2\text{V}_3\text{O}_8$ , and certain molecular magnets.<sup>32,33,34,35</sup> Within the rigid band scenario, the metal exchange process merely involves charge injection into the V  $3d$  conduction band, which is now partially-filled (see Fig. 3(d)).<sup>19</sup> The spectral response of the  $\text{Mn}^{2+}$ -substituted nanoscrolls in Fig. 2, however, clearly precludes the metallic state expected from the bandfilling model. Even if the partially-filled band of Fig. 3(d) is split due to chemical disorder effects (Fig. 3(e)), the resulting low energy excitation would be fairly broad due to joint density of states considerations in which the narrow occupied level below  $E_F$  is coupled to the wider empty conduction band arising from the V  $3d$  states.

We believe that the optical response indicates that the ion exchange process injects charges that are strongly localized due to disorder and Madelung energy considerations. Any charge introduced into the system can in principle reduce a  $\text{V}^{5+}$  to a  $\text{V}^{4+}$  ion. This extra electron remains pinned, however, as  $\text{Mn}^{2+}$  ions will “bind” preferentially (though not entirely) to the oxygen atoms bonded to a  $\text{V}^{4+}$  ion than to a  $\text{V}^{5+}$  ion, since proximity

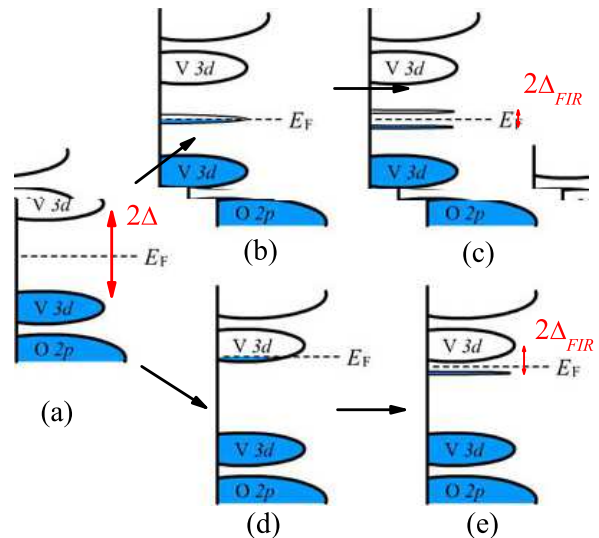


FIG. 3: (color online) Schematic representation of possible electronic structure changes resulting from the ion exchange process in the scrolled vanadates. (a) Band structure of pristine vanadium oxide nanoscrolls. Here,  $2\Delta$  denotes the  $\sim 0.5\text{ eV}$  optical gap.<sup>18</sup> (b) Schematic view in which ion exchange adds carriers to a new defect-level band that forms near  $E_F$ . (c) Cartoon view in which the new charge defect band splits due to the Madelung energy difference that exists in any charged system, electron-electron interactions, and/or chemical disorder effects. Here,  $2\Delta_{\text{FIR}}$  represents the pinned low-energy electronic excitation. This structure will likely have a relatively narrow bandwidth because the excitation is between split defect levels. (d) Alternate approach to the exchange process in which ion exchange adds carriers within the rigid band model.<sup>19</sup> A metallic state might be anticipated to arise from the partially-filled band. (e) Schematic view in which the V  $3d$  band splits due to chemical disorder effects. Here,  $2\Delta_{\text{FIR}}$  represents a possible low energy excitation, although it might be anticipated to display a wider band width than in scheme (c) due to joint density of states considerations.

to a  $\text{V}^{5+}$  ion would raise the Madelung energy substantially. Thus even in the “doped” system there exists a barrier to electron hopping between neighboring  $\text{V}^{4+}$  and  $\text{V}^{5+}$  ions. Within the effective band model therefore the charging process leads to strongly localized deep defect levels as shown in Fig. 3(b). The d.c. conductivity may be dominated by hopping between the disordered  $\text{V}^{4+}$  and  $\text{V}^{5+}$  ions. The nonbonding character of the localized levels gives them their narrow widths. The local potentials of the two kinds of ions continue to be different due to electron-electron repulsions between neighboring  $\text{V}^{4+}$ - $\text{V}^{4+}$  ions and long-range Madelung energy involving the  $\text{Mn}^{2+}$  ions. We have depicted this in Fig. 3(c) by an energy splitting between “occupied” (predominantly  $\text{V}^{4+}$ ) and “unoccupied” (predominantly  $\text{V}^{5+}$ ) defect levels. A dipole-allowed transition between these split defect levels would be consistent with a localized charge excitation

rather than a traditional metallic response in the low energy region of the optical conductivity. Such a feature would be relatively narrow, consistent with the 400 - 500  $\text{cm}^{-1}$  linewidth observed in the spectrum of  $\text{Mn}^{2+}$  substituted scrolls. The above localized picture is in better accord with our experimental results for the pristine and  $\text{Mn}^{2+}$  exchanged scrolls.

Careful examination of vibrational mode patterns can also provide information on the ion exchange process, although in this case, we must account for both charge and structural modifications. This analysis is possible because vibrational features are observed in both the pristine and ion exchanged materials. In the pristine vanadium oxide nanoscrolls, the mode at  $\sim 575 \text{ cm}^{-1}$  is assigned as the V-O-V equatorial stretch.<sup>18</sup> This mode is very sensitive to curvature, widening as the size of the amine template is reduced, characteristic of a more strained lattice.<sup>18</sup> The V-O-V equatorial stretching mode (Fig. 2) redshifts with ion substitution, moving from  $\sim 575 \text{ cm}^{-1}$  in the pristine scrolls, to  $\sim 570 \text{ cm}^{-1}$  in  $\text{Na}^+$  and  $\sim 560 \text{ cm}^{-1}$  in  $\text{Mn}^{2+}$  exchanged compounds. Similar shifts in peak position are also observed in other doped and intercalated vanadates.<sup>36,37</sup> From the structural point of view, the redshifted V-O-V equatorial stretching mode in the scrolled vanadates is unexpected because x-ray results indicate that the interlayer distance decreases as the smaller metal ions replace the larger amines.<sup>16</sup> The V-O-V equatorial stretching mode might therefore be expected to widen in the substituted scrolls due to their increased curvature, but the center peak position ought to be relatively insensitive to size.<sup>18</sup> Ion exchange also adds charge to the scrolls. We attribute changes in the V-O-V equatorial stretching mode position (Fig. 2) to charging effects which overcome the aforementioned local strain that tends to widen and slightly harden the V-O-V resonance. This overall softening trend ( $\sim 575 \text{ cm}^{-1}$  in the pristine scrolls to  $\sim 560 \text{ cm}^{-1}$  in the  $\text{Mn}^{2+}$  substituted compound) confirms that the ion exchange process adds carriers to the scrolls. The sharp, unscreened vibrational features in the ion substituted scrolls show, however, that the carriers are not mobile, consistent with the observation of a pinned charge excitation in the far infrared. The metal exchange process also leads to some chemical disorder, as evidenced in the splitting of a low frequency bending motion ( $\sim 179 \text{ cm}^{-1}$ ) and the screw-like mode of the scroll at  $\sim 112 \text{ cm}^{-1}$  that is analogous to the radial breathing mode in carbon nanotubes (inset, Fig. 2). Disorder in  $\text{Cu}^{2+}$  exchanged nanoscrolls has been reported recently as well.<sup>24</sup>

Figure 4 displays the 300 K optical conductivity of the pristine  $\text{VO}_x$  scrolls and the  $\text{Mn}^{2+}$  exchanged compound over a broader energy range. With the exception of the aforementioned bound carrier excitation localized in the far infrared (Fig. 2), the spectrum of the ion exchanged scrolls is similar to that of the pristine compound, in line with the fact that these excitations derive from the vanadium oxide framework.<sup>18</sup> Both materials display similar  $\sim 0.5 \text{ eV}$  optical gaps and excitations centered near 1 eV

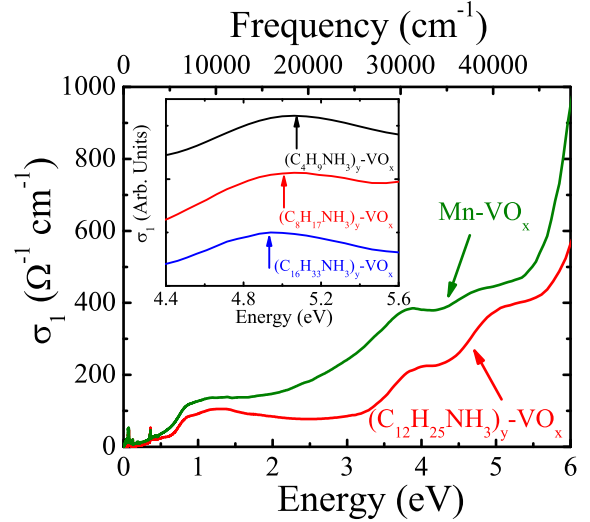


FIG. 4: (color online) Expanded view of the 300 K optical conductivity of pristine  $\text{VO}_x$  scrolls and the  $\text{Mn}^{2+}$  exchanged compound. The inset shows a close-up view of the  $\sim 5 \text{ eV}$  excitation, which changes modestly with sheet distance in the unsubstituted scrolls.<sup>18</sup> In the inset, the curves are offset for clarity.

that derive from a superposition of V  $d$  to  $d$  on-site excitations and  $\text{V}^{4+}$  to  $\text{V}^{5+}$  charge transfer excitations.<sup>18</sup> The O  $p$  to V  $d$  charge transfer excitations at  $\sim 3.9$  and  $\sim 5.0 \text{ eV}$  redshift with ion substitution. That this is a charge (rather than size) effect is evident from a comparison of the data in the inset of Fig. 4. Here, the excitation centered at  $\sim 5.0 \text{ eV}$ , which is probably polarized in the radial direction, shifts to higher energy as the size of the amine template decreases (corresponding to a reduction in the interlayer distance).<sup>18</sup> The  $3.9 \text{ eV}$  feature does not change with curvature.<sup>18</sup> The  $\text{Mn}^{2+}$  substituted scrolls display the opposite trend, indicating that charge effects also modify the charge transfer excitations. First principles electronic calculations will offer microscopic insight on this problem.

We measured the optical spectra of pristine and  $\text{Mn}^{2+}$  substituted vanadium oxide nanoscrolls in order to understand the charge dynamics in the pristine and metal exchanged materials and to test the applicability of the rigid band model. In contrast to expectations from the rigid band model, the spectra display a pinned low-energy electronic excitation in the  $\text{Mn}^{2+}$  substituted nanoscrolls rather than a traditional metallic response. We propose that the injected charge is localized due to disorder and Madelung energy effects. Our model is consistent with inhomogeneous charge disproportionation ( $\text{V}^{4+}$  and  $\text{V}^{5+}$ ) in both the pristine and the ion-exchanged materials, and explains the observed far infrared charge localization. Analysis of the vibrational properties shows that the  $575 \text{ cm}^{-1}$  V-O-V equatorial stretching mode redshifts with ion substitution, indicating that ion exchange mod-



ifies both the local curvature and charge environment. Charge effects also redshift two high energy electronic excitations.

### Acknowledgements

Work at the University of Tennessee is supported by the Materials Science Division, Office of Basic Energy

Sciences at the U.S. Department of Energy under Grant DE-FG02-01ER45885. Research at Binghamton is supported by the Division of Materials Research, National Science Foundation under Grant 0313963. Work at University of Arizona is supported by Materials Science Division, Office of Basic Energy Sciences at the U.S. Department of Energy under Grant DE-FG02-06ER46315. We thank H. Zhao for constructing Fig. 1(b).

- 
- \* Electronic address: musfeldt@utk.edu
- <sup>1</sup> C. N. R. Rao and M. Nath, *Dalton Trans.* **1**, 1 (2003).
  - <sup>2</sup> B. Halford, *Chem. and Eng. News* **83**, 30 (2005).
  - <sup>3</sup> R. Tenne, *Nature Nanotechnology* **1**, 103 (2006).
  - <sup>4</sup> M. J. Moses, J. C. Fetting, and B. W. Wichhorn, *Science* **300**, 778 (2003).
  - <sup>5</sup> Y. Wu, B. Messer, and P. Yang, *Adv. Mater.* **13**, 1487 (2001).
  - <sup>6</sup> F. Krumeich, H.-J. Muhr, M. Niederberger, F. Bieri, B. Schnyder, and R. Nesper, *J. Am. Chem. Soc.* **121**, 8324 (1999).
  - <sup>7</sup> H.-J. Muhr, F. Krumeich, U. P. Schönholzer, F. Bieri, M. Niederberger, L. J. Gauckler, and R. Nesper, *Adv. Mater.* **12**, 231 (2000).
  - <sup>8</sup> M. Wörle, F. Krumeich, F. Bieri, H.-J. Muhr, R. Nesper, *Z. Anorg. Allg. Chem.* **628**, 2778 (2002).
  - <sup>9</sup> C. O'Dwyer, D. Navas, V. Lavayen, E. Benavente, M. A. Santa Ana, G. González, S. B. Newcomb, and C. M. Sotomayor Torres, *Chem. Mater.* **18**, 3016 (2006).
  - <sup>10</sup> P. Y. Zavalij and M. S. Whittingham, *Acta. Cryst. B* **55**, 627 (1999).
  - <sup>11</sup> Y. Wang and G. Cao, *Chem. Mater.* **18**, 2787 (2006).
  - <sup>12</sup> M. Marezio, D. B. McWhan, P. D. Dernier, and J. P. Remika, *J. Solid State Chem.* **6**, 213 (1973).
  - <sup>13</sup> B. K. Chakraverty, M. J. Sienko, and J. Bonnerot, *Phys. Rev. B* **17**, 3781 (1978).
  - <sup>14</sup> T. Ohama, M. Isobe, H. Yasuoka, and Y. Ueda, *J. Phys. Soc. Jpn.* **66**, 545 (1997).
  - <sup>15</sup> M. Niederberger, H.-J. Muhr, F. Krumeich, F. Bieri, D. Günther, and R. Nesper, *Chem. Mater.* **12**, 1995 (2000).
  - <sup>16</sup> J. M. Reinoso, H.-J. Muhr, F. Krumeich, F. Bieri, and R. Nesper, *Helv. Chim. Acta* **83**, 1724 (2000).
  - <sup>17</sup> X. Wang, L. Liu, R. Bontchev, and J. Jacobson, *Chem. Commun.*, 1009 (1998).
  - <sup>18</sup> J. Cao, J. Choi, J. L. Musfeldt, S. Lutta, and M. S. Whittingham, *Chem. Mater.* **16**, 731 (2004); J. Cao, J. Choi, J. L. Musfeldt, S. Lutta, and M. S. Whittingham, *Nanoscale Materials: From Science to Technology*, Ch. 21, Nova Science Publishers (2006).
  - <sup>19</sup> L. Krusin-Elbaum, D. M. Newns, H. Zeng, V. Derycke, J. Z. Sun, and R. Sandstrom, *Nature* **431**, 672 (2004).
  - <sup>20</sup> S. Nordlinder, L. Nyholm, T. Gustafsson, and K. Edstrom, *Chem. Mater.* **18**, 495 (2006).
  - <sup>21</sup> J.-F. Xu, R. Czerw, S. Webster, and D. L. Carroll, *J. Balato*, R. Nesper, *Appl. Phys. Lett.* **81**, 1711 (2002).
  - <sup>22</sup> E. Vavilova, I. Hellmann, V. Kataev, C. Täschner, B. Büchner, and R. Klingeler, *Phys. Rev. B* **73**, 144417 (2006).
  - <sup>23</sup> S. Lutta, A. Doble, K. Ngala, S. Yang, P. Y. Zavalij, and M. S. Whittingham, *Mater. Res. Soc. Symp.* **703**, V8.3 (2002).
  - <sup>24</sup> A. G. Souza Filho, O. P. Ferreira, E. J. G. P. Santos, J. Mendes Filho, and O. L. Alves, *Nano. Lett.* **4**, 2099 (2004).
  - <sup>25</sup> F. Wooten, *Optical Properties of Solids* (Academic Press, New York, 1972).
  - <sup>26</sup> U. Fano, *Phys. Rev.* **124**, 1886 (1961).
  - <sup>27</sup> H. L. Liu, D. B. Tanner, H. Berger, and G. Margaritondo, *Physica C* **311**, 197 (1999).
  - <sup>28</sup> J. Choi, J. L. Musfeldt, J. He, R. Jin, J. R. Thompson, D. Mandrus, X. N. Lin, V. A. Bondarenko, and J. W. Brill, *Phys. Rev. B* **69**, 085120 (2004).
  - <sup>29</sup> Z.-T. Zhu, J. L. Musfeldt, Z. S. Teweldemedhin, and M. Greenblatt, *Phys. Rev. B* **65**, 214519 (2002).
  - <sup>30</sup> J. Cao, J. T. Haraldsen, R. C. Rai, S. Brown, J. L. Musfeldt, Y. J. Wang, X. Wei, M. Apostu, R. Suryanarayanan, and A. Revcolevschi, *Phys. Rev. B* **74**, 045113 (2006).
  - <sup>31</sup> H. Seo and H. Fukuyama, *J. Phys. Soc. Jpn.* **67**, 2602 (1998). M. V. Mostovoy and D. I. Khomskii, *Solid State Commun.* **113**, 159 (2000). P. Thalmeier and P. Fulde, *Europhys. Lett.* **44**, 242 (1998).
  - <sup>32</sup> H. W. Verleur, A. S. Barker Jr., and C. N. Berglund, *Phys. Rev.* **172**, 788 (1968).
  - <sup>33</sup> V. C. Long, Z. Zhu, J. L. Musfeldt, X. Wei, H.-J. Koo, M.-H. Whangbo, J. Jegoudez, and A. Revcolevschi, *Phys. Rev. B* **60**, 15721 (1999).
  - <sup>34</sup> J. Choi, J. L. Musfeldt, Y. J. Wang, H.-J. Koo, M.-H. Whangbo, J. Galy, and P. Millet, *Chem. Mater.* **14**, 924 (2002).
  - <sup>35</sup> A. Barbour, R. D. Luttrell, J. Choi, J. L. Musfeldt, D. Zipse, N. S. Dalal, D. W. Boukhvalov, V. V. Dobrovitski, M. I. Katsnelson, A. I. Lichtenstein, B. N. Harmon, and P. Kögerler, *Phys. Rev. B* **74**, 014411 (2006).
  - <sup>36</sup> E. Cazzanelli, G. Mariotto, S. Passerini, and F. Decker, *Solid State Ionics* **70-71**, 412 (1994).
  - <sup>37</sup> J. Choi, J. L. Musfeldt, G. Yu. Rudko, J. Jegoudez, and A. Revcolevschi, *Solid State Commun.* **123**, 167 (2002).